© 2018 IJSRSET | Volume 4 | Issue 6 | Print ISSN: 2395-1990 | Online ISSN : 2394-4099
Themed Section : Science and Technology

# Thermal Evolution of Magnesium Aluminate Spinel Nanoparticles Prepared By Coprecipitation Technique

**Dr. Shyam Sunder* and Dr. Wazir Singh**
Department of Applied Science & Humanities, Ch. Devi Lal State Institute of Engineering & Technology
Panniwala Mota, Sirsa, India
*Corresponding author: shyampph@yahoo.com

## ABSTRACT

$MgAl_2O_4$ spinel nanoparticles were prepared by coprecipitation method and followed by thermal heating at temperatures 550°C, 700°C, 850°C and 1000°C for 4 hours, in air. The samples were structurally characterized by TGA-TGT, XRD, FTIR and SEM with EDS. The effects of heat treatment on the structural properties of $MgAl_2O_4$ nanoparticles were investigated. The double hydroxide of magnesium and aluminium powders transformed from the amorphous phase, via intermediate cubic oxide ($\gamma$-$Al_2O_4$, a rock salt type structure) disordered phase, into face-centred cubic $MgAl_2O_4$ spinel nanoparticles. In a low calcination temperature range 700-850°C for 4h, $MgAl_2O_4$ face-centred cubic disordered spinel nanoparticles with grain size ~ 6 nm is obtained. At 1000°C (4h), disorder-order phase transformation results in a sudden increase in the lattice increased constant. Single phase $MgAl_2O_4$ cubic ordered-spinel nanoparticles (grain size ~ 12 nm) with a good chemical homogeneity, narrow particle size distribution are obtained. It is also shown that heat treatment enhances the crystallinity and transmission of the spinel; and also controls dislocation density and amount of stress at the surface and hence yields the strength of the material. Results of FTIR and SEM support XRD studies. The realization of temperature dependent structural properties makes the applicability of the $MgAl_2O_4$ nanocrystalline powders more versatile.

**Keywords** : Magnesium Aluminate, Nanoparticle, Coprecipitation, Structure Characterization

## I. INTRODUCTION

Magnesium aluminate ($MgAl_2O_4$) spinel, as one of the important ceramic materials, finds wide applications in metallurgical, chemical and electrical industries because it possess unique combination of desirable properties such as high melting point (2135°C), good mechanical strength at room and elevated temperatures, high chemical inertness and good shock resistance [1-2]. Magnesium aluminate ceramic have been used as: refractory in heavy industry, substrate for solid-state electronic devices, ceramic ultra-filtration membranes and fibre-optic temperature sensors etc. [3-7]. For many of its applications, in particular as catalyst support and catalysts by itself, a high surface area, small crystalline size and special active sites are greatly desired [8] $MgAl_2O_4$ spinel nanoparticles more or less fulfil the aforesaid demands. $MgAl_2O_4$ is a mixed oxide and its physical properties range between those of MgO and AlO. Physical properties of nanometric magnesium aluminate spinels are strongly dependent on the method of preparation and experimental conditions [9-10]. In order to synthesize $MgAl_2O_4$ spinel nanoparticles with high purity, chemical homogeneity, fine particle size, narrow particle size

distribution, and less particle agglomeration with high sinter activity several methods have been used and each method has its own advantages and limitations [11]. Ball milling method introduces impurity in the spinel nanoparticles which restrict further implementation of the product [12]. $MgAl_2O_4$ spinel nanoparticles were obtained at high temperatures 1200°C by using freezing drying and heterogeneous wet chemical sol–gel techniques [13-14]. Spinel powders synthesized by solgel of metal alkoxides are usually characterized by high reactivity and less agglomeration. However, metal alkoxides are expensive and most of the solvents for them are toxic. Besides, special measures are required during manipulating alkoxide materials due to their high sensitivity to the moisture in air. Recently, nanosized $MgAl_2O_4$ spinel powders were synthesized by other wet chemical methods like nitrate citrate auto-ignition [15], solgel-citrate method and followed by a heat treatment in a continuous air and argon flow (40ml/min) [16], coprecipitation method in presence of ZnO or MnO as additives [17] and 8-hydroxyquinoline (HQ) and tetraethyl ammonium hydroxide (TEAOH) as organic precipitating agents [7]. Amongst them, the coprecipitation method is a cost effective technique and suitable for the mass production of homogenous, fine and reproducible nanocrystallites with narrow size distribution at relatively low reaction temperature [7]. In addition, sinterability of a coprecipitation derived oxide powder has close relationship with the properties of its precursor. In these studies, a phase transformation in $MgAl_2O_4$ spinel has not investigated.

In this work, $MgAl_2O_4$ cubic spinel nanoparticles have been synthesized by co-precipitation method and followed by thermal treatment at different temperatures 550°C, 700°C, 850°C and 1000°C for 4h in air. Effects of heat treatment on structural evolution, lattice constant micro-strain and grain size of magnesium aluminate powders have discussed in detail. The as-prepared powders were amorphous and upon heating at 500°C (4h) decomposed into intermediate products γ-$Al_2O_3$ (a rock salt type structure) and MgO, in which γ-$Al_2O_3$ contains both tetrahedral and octahedral aluminium with incipient spinel. We have explored a possibility of thermal induced rock salt-to-spinel structural (disorder-order) phase transformation in magnesium aluminate nanoparticles prepared by coprecipitation method. It is found that degree of order phase in $MgAl_2O_4$ spinel nanoparticles increases with increasing calcination temperature. A well formed $MgAl_2O_4$ cubic ordered-spinel nanoparticles (grain size ~12 nm) with a good crystallinity, chemical homogeneity, densification, and narrow particle size distribution have been obtained at calcination temperature 1000°C for 4 hours.

## II. EXPERIMENTAL

$Mg(NO_3)_2{\cdot}6H_2O$ (99.99% purity Sigma Aldrich ACS grade), $Al(NO_3)_3{\cdot}9H_2O$ (99.99% purity Sigma Aldrich ACS grade) and ammonia solution (Sigma Aldrich, 28%, ACS grade) were used as reagents. A 0.2 M solution of the nitrates was prepared, with Mg:Al (molar ratio) = 1:2. The precursor was prepared by slowly adding the mixed salt solution into the ammonia solution under rigours stirring, pH was maintained around 8-9 and reaction temperature was maintained at 60°C. The precursor were washed with an excess of double distilled water, and dried for 24 hrs at 100°C in an oven. The solid so-obtained was grinded in agate mortar pestle. Furthermore, powdered samples were calcined at different temperatures 550°C, 700°C, 850°C and 1000°C in presence of air. In all calcination schedules, heating rate was 10°C $min^{-1}$ and incubation time was 4 hours. Thermo Gravimetric and Differential Thermo Gravimetric Analysis (TGA-DTG) were carried out in Mettler Toledo equipment, model TGA/SDTA851e. Powdered sample was heated from room temperature up to 1000°C in air flow with a 10°C $min^{-1}$. X-ray diffraction experiments were performed at room temperature in a Rigaku Miniflex-II instrument using CuKα radiation (λ = 1.5406 Å), generated at 30 kV and a current of 15 mA. The morphology and microstructure of the powders was studied by

scanning electronic microscope (SEM), with a Nova NanoLab 200 FEG-SEM/FIB, equipped with EDS.

## III. RESULTS AND DISCUSSION

### 3.1 TGA/DTG

The reaction pathways in the formation of magnesium aluminate are determined with the thermal analysis. TGA-DTG curves of the powdered sample are shown in Figure 1. The TG curve shows a major weight loss of the sample at four different temperatures range 35-170°C, 171-270°C and 271-500°C and 501-800°C.

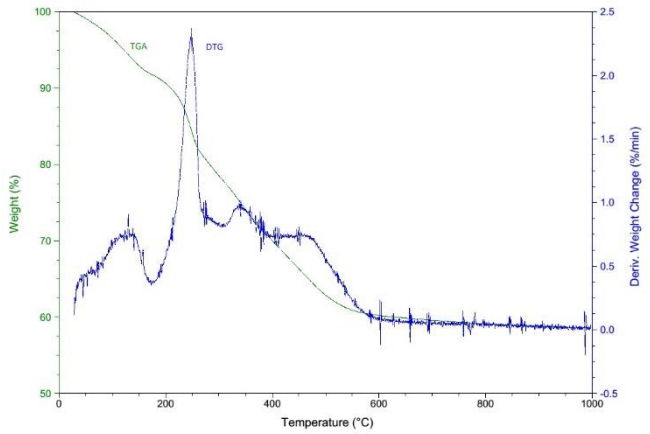


**Fig. 1.** The TGA-DTG curves of the magnesium aluminate powder.

Between temperatures 35-170°C (first stage), the weight loss is 8.0% corresponding to loss of free water molecules. Over a temperature range 171-250°C (second stage), the weight loss is nearly 11% and this weight loss could be due to decomposition of precursors. In DTG curve, a strong peak around temperature 220°C is evident and it could be due to decomposition of double hydroxide of magnesium and aluminium [18]. Between the temperatures range 271-500°C (third stage); the rate of weight loss is almost constant, indicating an intermediate structure is formed. Over a temperature range 501-800°C, the weight loss is very small implying no change in phase of the structure. Finally, between temperatures 801 and 1000°C curves exhibit negligible weight loss in the sample, indicating a stable structure of the magnesium aluminium oxides is formed.

### 3.2 XRD

Diffraction pattern of the as-prepared and calcined samples is shown in Figure 2. Diffraction pattern of the as-prepared sample (a) depicts broad peaks around 2θ~18.40° and 20.28° which could be the peaks of double hydroxide of magnesium and aluminium (JCPDS Card No. 35-1274). The formation of double hydroxide is important in coprecipitation method because upon heating double hydroxide decompose in a spinel structure product [17, 19].

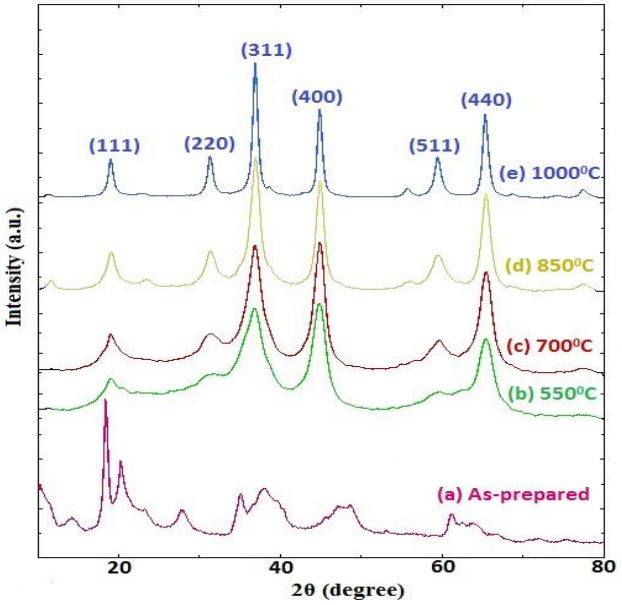


**Fig. 2** XRD patterns of as-prepared and thermally treated samples of magnesium aluminate at different temperatures for 4h.

XRD pattern of the sample calcined at 550°C shows the peaks of double hydroxide is vanished but four new broad peaks are appeared at 2θ ~ 19.02°, 36.86°, 44.84°, 65.44° and these new peaks could be assigned peaks of γ -$Al_2O_4$ (JCPDS 77-0396), which is an intermediate phase of cubic spinel structure [20]. This result supports corresponding TGA/DTG data and also gives confidence that $MgAl_2O_4$ cubic spinel nanoparticles could be synthesized by the coprecipitation method and followed by calcination at moderate temperatures. When the sample was calcined at 700°C, an increase in the intensity of the

diffraction peaks at 2θ ~ 36.86°, 44.84°, 65.44° was observed. In addition, new broad peaks at 2θ~31.34° and 59.52° were also noticed. When calcination temperature was increased up to 850°C, the increase in the peaks height accompanied by sharpening in characteristics diffraction peaks (2θ ~ 19.02°, 31.34°, 36.86°, 44.84°, 59.52°, 65.42°) of spinel phase was observed.

**Table-1**

| Calcined Sample | Crystallite size $D_{W-H}$ (nm) | Strain ($\varepsilon$) | Lattice constant (Å) | X-ray density $\rho_{XRD}$ (g/cm³) | Dislocation density $\rho \cong \frac{1}{D_{XRD}^2}$ | Degree of ordered phase |
|---|---|---|---|---|---|---|
| 550°C(4h) | 6.29 | 8.65x10⁻³ | 8.0660 | 3.250 | 0.02527 | 0.734 |
| 700°C(4h) | 5.82 | 2.62 x10⁻³ | 8.0600 | 3.257 | 0.02954 | 0.738 |
| 850°C(4h) | 6.04 | 0.07 x10⁻³ | 8.0593 | 3.246 | 0.02742 | 0.833 |
| 1000°C(4h) | 11.8 | 1.76 x10⁻³ | 8.0669 | 3.249 | 0.00718 | 0.971 |

Diffraction peaks are compared with the standard data of face centred cubic $MgAl_2O_4$ (JCPDS Card No. 21-1152) and found in accordance with the diffraction peaks of the standard data and the diffraction peaks are indexed by Miller indices (111), (311), (400), (511), (400), respectively. This result suggests that interfacial interaction between a high reactive decomposed product γ-$Al_2O_3$ and MgO and their mixing at molecular level at temperature 700°C (4h), yields a spinel phase. Here, it is worth mentioning that the characteristics peaks of $MgAl_2O_4$ in samples (c) and (d) are slightly shifted toward higher value of Bragg's angle, which imply: (i) a decrease in lattice constant [21] and (ii) an increase in intrinsic nature of atomic thermal vibration in face centred cubic $MgAl_2O_4$ [22]. In order to get details of the structural and microstructure parameters of the prepared $MgAl_2O_4$ spinel nanoparticles, diffraction data are further examined. Effects of heat treatment on structure parameter of $MgAl_2O_4$ like lattice constant, spinel phase, crystallites size and microstrain and dislocation density have been discussed. In general, the lattice constant of crystalline material is obtained by inter planner distance and Miller indices.

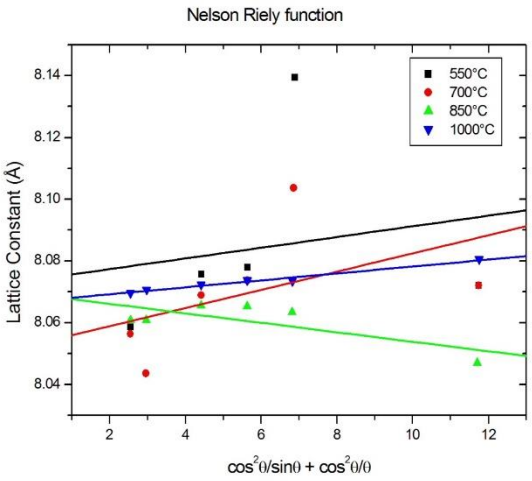


**Fig. 3** Lattice constant versus Nelson-Riley function.

In this work, lattice constant of $MgAl_2O_4$ crystallites is calculated by Nelson-Riley function, because this function eliminates the error in lattice constant due to sample displacement [23] Figure 3 displays lattice constant versus Nelson-Riley function. Value of lattice constant for different calcination temperatures is obtained from the intercept of the straight line and represented in Table-1. It is noticed that lattice constant of $MgAl_2O_4$ calcined powders is smaller than that of the bulk and this could be due to size effect [24]. Figure 4 exhibits a change in lattice constant (see Y-axis at Right hand) of $MgAl_2O_4$ spinel nanoparticles with increasing calcination temperature. Lattice constant shows a decreasing trend (8.0660 to 8.0593 Å) from the calcination temperature 550°C to 850°C for 4 hours. In general, tetrahedral and octahedral interstitial sites of spinel are not fully occupied by their respective divalent and trivalent cations and they enter into the interstitials sites as defective cations.

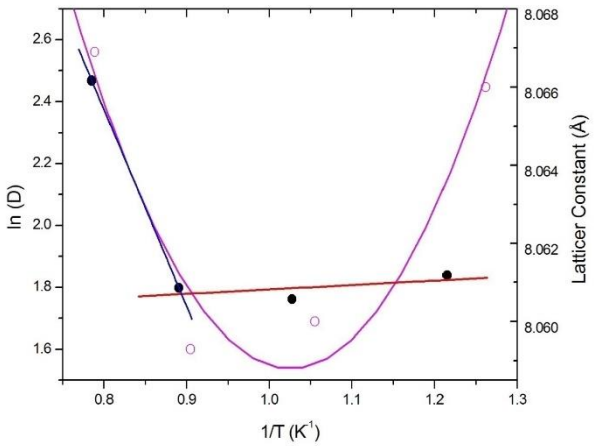


**Fig. 4** Crystallite size ( Left hand side-axis) and lattice constant (Right hand side-axis) versus calcination temperatures for 4 h.

The divalent ions are generally larger than the trivalent ions where as tetrahedral sites are smaller than the octahedral sites. Therefore, it would be reasonable that the trivalent ions could go into the tetrahedral / octahedral sites or into both sites where as the divalent ions would prefer to go into the octahedral sites. It is expected that at low calcination temperature 550°C (4h), a fraction of $Mg^{2+}$ (average ionic radius ~ 0.78 Å) and $Al^{3+}$ (average ionic radius ~ 0.45 Å) cations occupy their respective sites and remaining cations $Mg^{2+}$ and $Al^{3+}$ occupy spinel interstitial sites as impurity cations. As the calcination temperature is increased from 550°C to 850°C, impurity cations (magnesium ions) migrate from octahedral to tetrahedral sites whereas another impurity cations (aluminium ions) migrate from tetrahedral to octahedral sites. The cations distribution among the interstitial sites has competing effects because of a large difference between average ionic radius of $Mg^{3+}$ and $Al^{3+}$ cations. Al ions (being smaller than the Mg ions) migrate comparatively faster than the Mg ions. As the tetrahedral sites are of too small for the divalent ions so that the oxygen ions move slightly to accommodate them. The oxygen ions connected with the octahedral sites move in such a way as to shrink the size of the octahedral cell by the same amount as the tetrahedral site expands and as a result lattice constant decreases. In addition, calcination temperature (550°C to 850°C for 4h) is not sufficient for migration of all Mg cations (impurity cations) from the octahedral sites to tetrahedral sites and therefore a few tetrahedral sites are remain unoccupied. The decreasing trend in lattice constant and an inequity distribution of cations among interstitials sites could be responsible mechanisms for disordering in $MgAl_2O_4$ spinel nanoparticles. Moreover, in these experimental conditions, a decrease in lattice constant hence lattice volume indicates that most of the atoms on the surface of disordered spinel and hence surface effects and lattice strain are obvious in such spinels. Simone et al observed a clear shift of the unit cell parameter on the irradiated samples $MgAl_2O_4$ [25]. Sikafus et al. reported chemically induced disorder in $MgAl_2O_4$ due to dispalacive transformation in which atoms move to forbidden sites [26]. In our studies, at relatively higher calcination temperature 1000°C (4h), the lattice constant is suddenly increased and is found to be 8.0669 Å. A sudden increase in lattice constant of $MgAl_2O_4$ spinel nanoparticles indicates a disorder-order phase transition in $MgAl_2O_4$ [27]. In this experimental condition, there is sufficient energy which enables both the cations to migrate between the two interstitial sites and nearly an equilibrium cations distribution is expected. The migration of these cations between the interstitial sites continues unless its free energy attains a minimum value. Similar behaviour has been observed in $MgFe_2O_4$ [3, 11, 28]. The present study provides a milder experimental condition than the ion beam irradiated treatment, the existence of disorder spinel structure has been observed in our calcined samples and this could be due to different ions size and temperature dependent distribution of defective ions among the interstitial sites. Further, a fraction of ordered phase in spinel $MgAl_2O_4$ nanoparticles has been estimated by comparing the peak intensity of (311) and (400) reflections by using the literature [29-30]:

$$\text{Degree of order in the spinel powders} = \left[\frac{I_O}{(I_O + I_D)}\right] \quad (1)$$

Where $I_O$ = intensity of {311} plane (order phase); $I_D$ = $I_{C,400} - I_{O,400}$ = intensity of disorder spinel phase in {400} plane; $I_{C,400}$ = intensity of {400} plane having both order and disorder phase; and $I_{O,400}$ = intensity of order phase in {400} plane. All the intensity values used in this calculation were absolute intensities (cps) after subtracting the background intensity. As expected, a low degree of ordered phase is found in the sample calcined at 550°C and 700°C (4h). When the sample was calcined at temperature 800°C and 1000°C for 4h, an increase in relative intensity of odd reflections (311) is clearly evident in the XRD pattern this could be growth of a plane in preferred direction, while the relative intensity of even reflections (400) decreases because of lower intensity of (200) disordered reflections. The change in the representative peak intensity confirms disorder-order transition in $MgAl_2O_4$ spinel nanoparticles [30]. The estimated degree of order in the spinel nanoparticles is given in Table 1. The data clearly reveal that the degree of order in $MgAl_2O_4$ spinel nanoparticles increases when the samples were calcined in the temperature range of 700-1000°C.

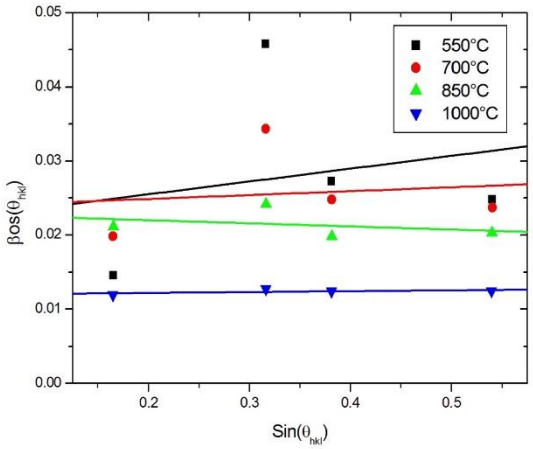


**Fig. 5** Williamson-Hall (W-H) plot of calcined of $MgAl_2O_4$ spinel nanopowder

To this end, effects of calcination temperature on grain size and micro-strain of $MgAl_2O_4$ spinel nanoparticles have also been investigated. The crystallite size and micro-strain produces peak broadening in the diffractogram. This could be due to the stresses and faults inside the prepared spinel nanoparticles. The crystallite size and the strain effect have to be differentiated in the diffractogram. Both effects are independent and can be distinguished by size-strain plot (W-H plot). Using W-H plot, size and micro-strain of the crystallite are estimated simultaneously. The W-H equation is:

$$\beta_{hkl}Cos(\theta_{hkl}) = \frac{K\lambda}{D_{WH}} + 2\varepsilon Sin(\theta_{hkl}) \quad (2)$$

Where K is the shape factor, λ is the wavelength of X-ray, $\theta_{hkl}$ is the Bragg angle, ε is the micro-strain and $D_{W-H}$ is average crystallite size measured in a direction perpendicular to the surface of the specimen. The graph is plotted between $Sin(\theta_{hkl})$ and $\beta_{hkl}Cos(\theta_{hkl})$ as shown in Figure 5. The value of micro-strain is obtained from slope of the fitted line, whereas value of crystallite size is obtained from the intersection with the vertical axis. By fitting the data, the average crystallite size ($D_{W-H}$) and micro-strain (ε) are estimated and given in Table 1. The grain size and micro-strain do not change significantly in the calcination temperature range 550°C to 850°,C for 4 hour, however at 1000°C (4h) a significant increase in crystallite size and decrease in micro-strain is are found. Crystallite size (see Y-axis at Left hand) versus calcination temperature is shown Figure 4. Growth of crystallite size with respect to calcination temperature is not linear and thus heat treatment could be divided in a low calcination temperature range and higher calcination temperature. In low calcination temperature range (550-850°C for 4h), disordered $MgAl_2O_4$ cubic spinel nanoparticles were obtained and the activation energy for the formation found this phase is found to be 1.2 kJ/mol. The calcination at relatively higher temperature (1000°C) yielded ordered $MgAl_2O_4$ cubic spinel nanoparticles and the activation energy for formation of ordered phase is found to be 53 kJ/mol. A rapid increase in crystallite size could be due to coalesces of nanopraticles and grain boundary migration and is accompanied by higher activation energy [31]. Further, by knowledge of average crystallite size and an empirical relation

$\rho \cong \frac{1}{D_{XRD}^{\ 2}}$ , dislocation density of $MgAl_2O_4$ cubic spinel nanocrystallites is obtained and given in Table-1. As calcination temperature is increased, the density of dislocation decreased as a result of less nucleation sites being available during crystallization upon heating, which in turn lead to the comparatively larger final crystallite size.

### 3.3 FTIR

FTIR Spectroscopy provides valuable information about the phase composition and bonding in the samples. The FTIR of (a), (b), (c) and (d) samples is shown in Figure 6 within the spectral range of 4000-400 $cm^{-1}$. FTIR spectrum of as-prepared sample shows three distinct strong absorption bands centered around 1333, 1636 and 3461 $cm^{-1}$. The absorption band centred around 1333 $cm^{-1}$ could be ascribed presence of nitrate groups [32]. The bands around 3461 $cm^{-1}$ and 1641 $cm^{-1}$ and could be assigned as the stretching vibration of H-O-H molecule and the bending modes of H-O-H absorbed at surface of the product, respectively [33].

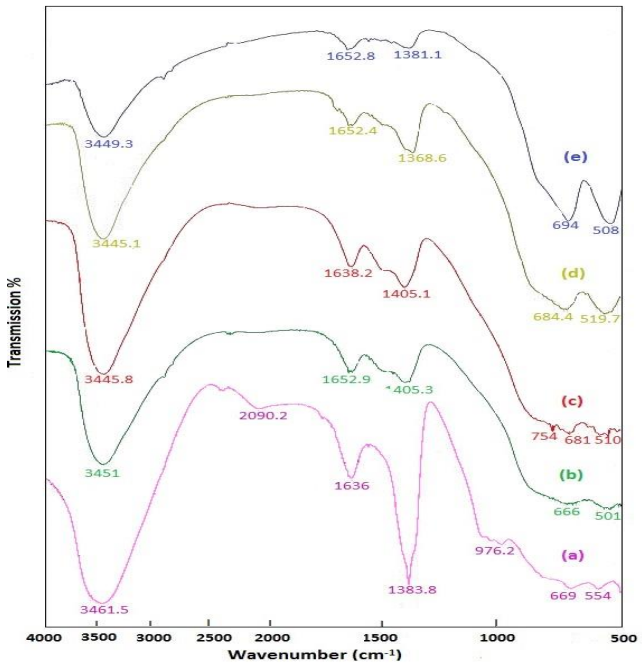


**Fig. 6.** FTIR spectra of as-prepared and thermally treated samples of magnesium aluminate at different temperatures for 4h.

The stretching vibration of H-O-H molecules overlaps with surface hydroxyl group vibrations and as a result the stretching band broadens [34]. In FTIR spectroscopy, the bands over range of 1000-400 $cm^{-1}$ are assigned by metal oxygen bonds (M-O-M) [10]. Narrow bands noted around 669 and 554 $cm^{-1}$ may be assigned as double hydroxide of magnesium and aluminium [35]. FTIR of Sample (b) shows two distinct signatures : (i) an evaporation of nitrate group which is manifested by elimination of the absorption band centred around 1333 $cm^{-1}$ and this signature confirms decomposition of nitrates; (ii) broadening in the double hydroxide band. When calcination temperature was increased up to 700°C and hold for 4h, bands of double hydroxides almost disappeared but new weak bands appeared around $\nu_1$=725, $\nu_2$=690 and $\nu_3$=505 $cm^{-1}$, which could be assigned $AlO_4$ group [36], $AlO_6$ group and Mg-O stretching vibrations, respectively [28, 37]. This result supports XRD data and confirms the presence of some of $Al^{3+}$ in both the tetrahedral and octahedral sites. The presence of Al cations (impurity/defects) in the tetrahedral sites leads to local structural disorder in $MgAl_2O_4$ spinel nanoparticles. As the calcination temperature was increased up to 850°C, the absorption band of $AlO_6$ and MgO become stronger and evaporation surface water molecules increases as well but absorption band of $AlO_4$ diminishes. However, at relatively higher calcination temperature of 1000°C (4h), the appearance of the tetrahedral and octahedral sites band becomes sharper due to the minimization of lattice distortion and enhancement of crystallinity (reduction of surface effect). The increase in calcination temperature shifts the position of the $\nu_1$ and $\nu_2$ bands, which might be attributed to the changes that occurred in the cation distribution (i.e. migration of cations from tetrahedral to octahedral sites and vice versa) and variations in the cation-oxygen bond length for octahedral and tetrahedral complexes [35]. At calcination temperature 1000°C, the increase in frequency of $\nu_1$ band arise due to size effect and the decrease in frequency of $\nu_2$ may arise due to the repulsive dipolar interactions [38]. The FTIR results are in close agreement with XRD studies.

Here it is worth pointing out that even at higher calcination temperature 1000°C for 4 hours, some OH groups (3450 $cm^{-1}$ and 1640 $cm^{-1}$) remains in the structure. This small amount of water molecules could be due to the inter absorption during the compaction of powder specimen with KBr.

### 3.4 SEM

The surface morphology of the as-prepared and calcined samples was investigated by SEM equipped with EDS and shown in Figure 7a & 7b.

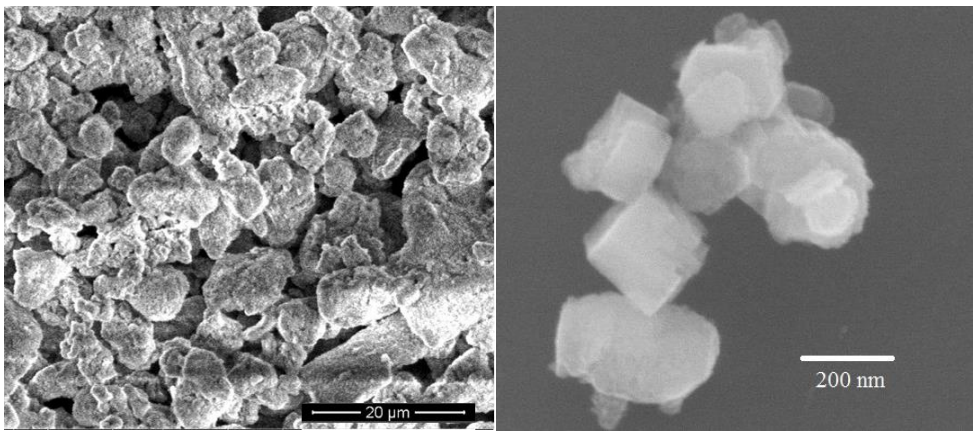


1000

Fig. 7d SEM micrographs of $MgAl_2O_4$ spinel, at temprature 1000°C:(e).

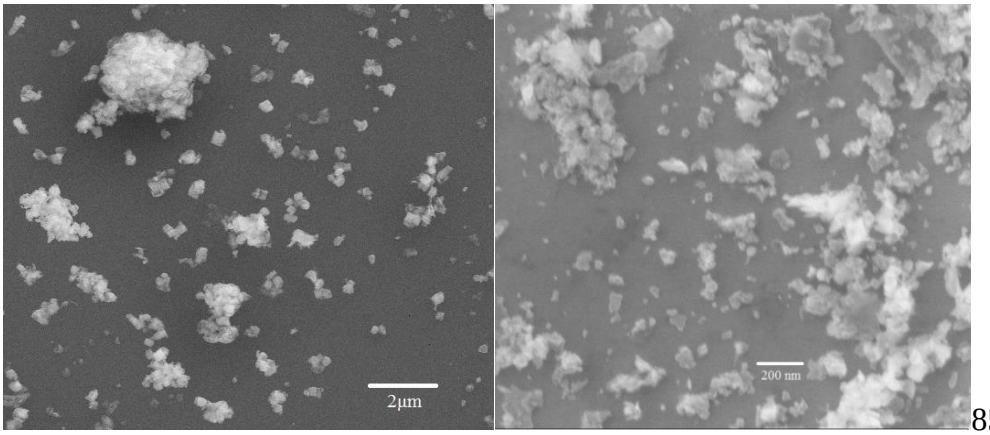


850

Fig. 7c SEM micrographs of $MgAl_2O_4$ spinel, at temprature 850°C.

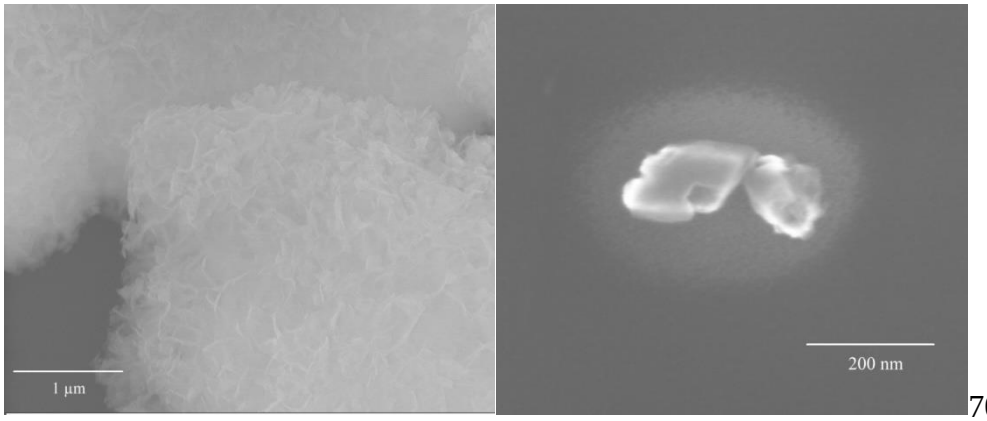


700

Fig. 7b SEM micrographs of $MgAl_2O_4$ spinel, at temprature 700°C

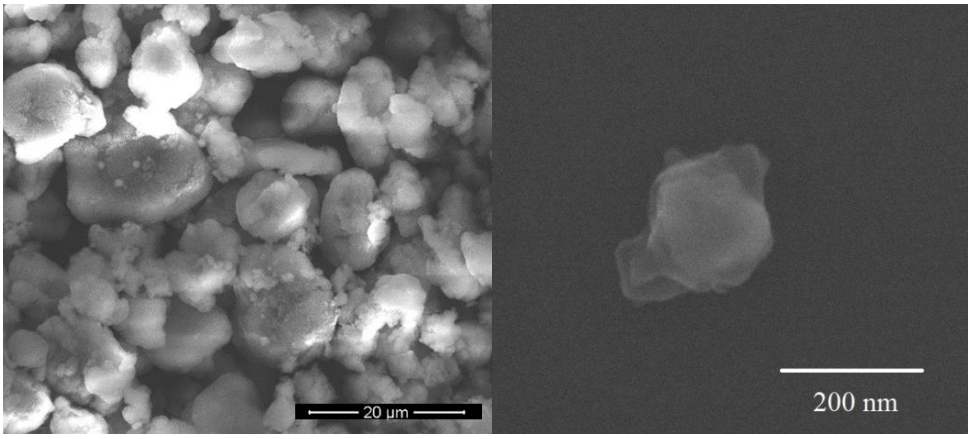


Fig. 7a SEM micrographs of $MgAl_2O_4$ spinel as preapred.

The micrograph (a) reveals that coprecipitation method produces almost spherical shape microstructured precursors. At calcined temperature 700°C, morphology of the precursors turned into globular shape structure and at temperature 850°C clusters of spherical nanopraticles was formed. The micrograph of the sample calcined at 1000°C for 4h, reveals stratified structure of $MgAl_2O_4$ spinel nanoparticles with good densification and this structure could have formed by coalesces of rectangle shape microparticles. Figure 8 illustrates the EDS spectrum of the samples and confirms the presence of magnesium, aluminium and oxygen.

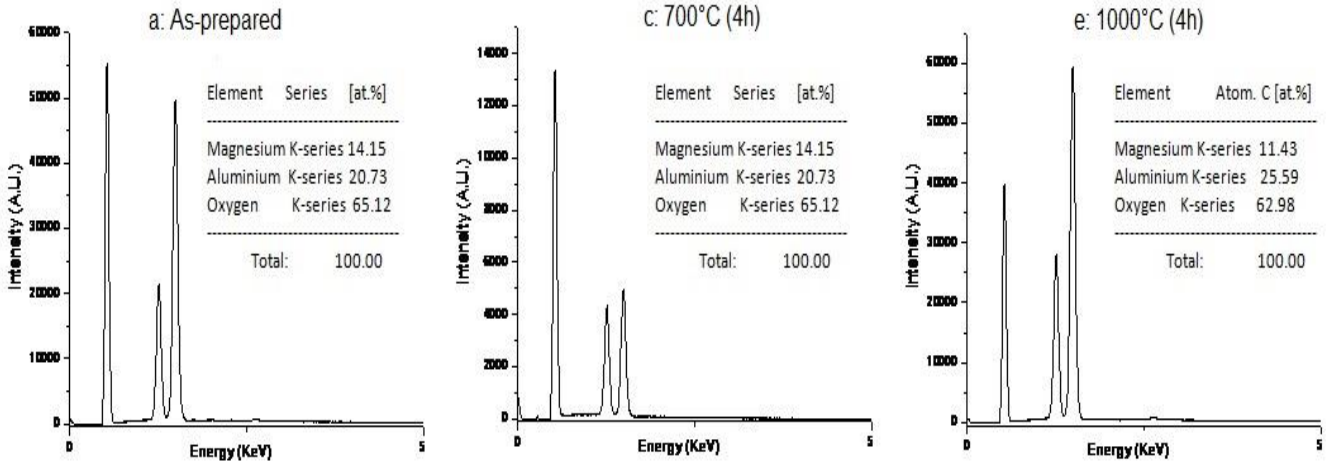


**Fig. 8** EDS of samples as preapred: (a), temprature 700°C: (c) and temprature 1000°C: (e)

There is an excess of both Al and O ions relative to Mg ions, in $MgAl_2O_4$ spinel nanoparticles. Note in case of the sample annealed at 1000°C, the peak intensities of the EDS spectrum revealed atomic ratio of Mg:Al is approximately 1:2.

## IV. SUMMARY

In summary, using precursors: $Mg(NO_3)_2{\cdot}6H_2O$, $Al(NO_3)_3{\cdot}9H_2O$ and ammonia solution, as a catalyst, $MgAl_2O_4$ nanoparticles were prepared by coprecipitation method and subsequent thermal heating at temperatures 550°C, 700°C, 850°C and 1000°C for 4 hours, in air. The structural properties of $MgAl_2O_4$ nanoparticles were investigated by techniques TGA/TGA, XRD, FTIR and SEM. XRD investigations revealed that at calcination temperature 550°C, an intermediate phase ($\gamma$-$Al_2O_4$ , a rock salt type structure) of cubic $MgAl_2O_4$ was formed. In low calcination temperature range (700-850°C 4h), interfacial interaction between a high reactive

decomposed products γ-$Al_2O_3$ and MgO and their mixing at molecular level yielded $MgAl_2O_4$ face-centred cubic spinel nanoparticles with grain size ~ 6 nm via distribution/ inversion of cations among/between the interstitial sites. In addition, a decrease in lattice constant suggests that a disordered character of the cubic spinel phase. At 1000°C, results shows that the lattice constant is suddenly increased due to disorder-order phase transition and found $MgAl_2O_4$ cubic spinel nanoparticles (size 12 nm) with degree of ordered 0.97. The distribution/exchange of cations among /between the interstitial sites depends on average ionic radius of cations and calcination temperatures. The study also suggests that nearly 44 times more energy is required for formation of $MgAl_2O_4$ face-centred cubic ordered-spinel nanoparticles than that of $MgAl_2O_4$ cubic disordered-spinel nanoparticles. It is also shown that calcination enhances the crystallinity and transmission of the spinel; and also controls dislocation density and amount of stress at the surface and hence yields the strength of the material. Results of FTIR and SEM support XRD studies. Finally, we may conclude that a single phase $MgAl_2O_4$ cubic ordered-spinel nanoparticles (grain size ~ 12 nm) with a good, chemical homogeneity (atomic ratio of Mg:Al is approximately 1:2), narrow particle size distribution can be obtained by using co-precipitation method and followed by thermal treatment at temperature 1000°C for 4h, in air; and may be used for applications: refractory in heavy industry nano ceramic powders in particular as catalyst support and catalysts by itself.

## V. REFERENCES


1. J-G Li, T Ikegami, J-H Lee, T. Mori, Y. Yajima, A wet-chemical process yielding reactive magnesium aluminate spinel (MgAl2O4) powder, Ceram. Int. 27 (2001) 481-489.
2. C. Baudin, R. Martinez, P. Pena, High-temperature mechanical behaviour of stoichiometric magnesium spinel, J. Am. Ceram. Soc. 78 (1995) 1857–1862.
3. M. A. Sainz, A. Caballero, Aluminium oxycarbide formation on carbon-coated Al2O3-MgO spinel, Key. Engg. Mater. 132–136 (1997) 846–847.
4. J.G. Li, T. Ikegami, J.H. Lee, T. Mori, Fabrication of translucent magnesium aluminium spinel ceramics, J. Am. Ceram. Soc. 83 (2000) 2866–2868.
5. G. Gusmano, G. Montesperelli, E. Traversa, G. Mattogno, Microstructure and electrical properties of MgAl2O4 thin films for humidity sensing, J. Am. Ceram. Soc. 76 (1993) 743–750.
6. L. Thome, A. Gentils, J. Jagielski, F. Garrido, T. Thome, Radiation stability of ceramics: Test cases of zirconia and spinel, Vacuum 81 (2007) 1264–1270.
7. M.M. Rashad, Z.I. Zaki, H. El-Shall, A novel approach for synthesis of nanocrystalline MgAl2O4 powders by co-precipitation method, Mater. Sci. 44 (2009) 2992–2998.
8. C.W. Fairhurst, Dental Ceramics: the State of the Science, Adv. Dent. Res. 6 (1992) 78–81.
9. H. Revero´n, D. Gutie´rrez-Campos, R.M. Rodrı´guez, J.C. Bonassin, Chemical synthesis and thermal evolution of MgAl2O4 spinel precursor prepared from industrial gibbsite and magnesia powder, Mater. Lett. 56 (2002) 97-101.
10. J. Parmentier, M. Richard-Plouet, S. Vilminot, Influence of the sol-gel synthesis on the formation of spinel MgAl2O4, Mater. Res. Bull. 33 (1998) 1717-1724.
11. B. Alinejad, H. Sarpoolaky, A. Beitollahi, A. Saberi, S. Afshar, Synthesis and characterization of nanocrystalline MgAl2O4 spinel via sucrose process, Mater. Res. Bull. 43 (2008) 1188-1194.
12. H.J. Fecht, Formation of nanostructured by mechanical attrition. In: A.S. Edelstein, R.C. Cammaratra (2nd edn), Nanomaterials: Synthesis, Properties and Applications, Taylor & Francis Group LLC, 1996, pp. 89-95
13. C.T. Wang, L.S. Lin, S.J. Yang, Preparation of MgAl2O4 Spinel Powders via Freeze-Drying of

Alkoxide Precursors, J. Am. Ceram. Soc. 75 (1992) 2240-2243.
14. T. Shiono, K. Shiono, K. Miyamoto, G. Pezzotti, Synthesis and Characterization of MgAl2O4 Spinel Powder from a Heterogeneous Alkoxide Solution Containing Fine MgO Powder, J. Am. Ceram. Soc. 83 (2000) 235–237.
15. S.K. Behera, P. Barpanda, S.K. Pratihar, S. Bhattacharyya, Synthesis of magnesium-aluminium spinel from autoignition of citrate-nitrate gel, Mater. Lett. 58 (2004) 1451-1455.
16. A. Saberi, F. Golestani-Fard, M. Willert-Porada, Z. Negahdari, C. Liebscher, B. Gossler, A novel approach to synthesis of nanosize MgAl2O4 spinel powder through sol–gel citrate technique and subsequent heat treatment, Ceram. Int. 35 (2009) 933–937.
17. M.F. Zawrah, H. Hamaad, S. Meky, Synthesis and characterization of nano MgAl2O4 spinel by the co-precipitated method, Ceram. Int. 33 (2007) 969-978.
18. P. Ku´strowski, A. Rafalska-Lasocha, D. Madja, D. Tomaszewska, R. Dziembaj, Preparation and characterization of new Mg–Al–Fe oxide catalyst precursors for dehydrogenation of ethylbenzene in the presence of carbon dioxide, Solid State Ionics 141–142 (2001) 237-242.
19. S.A. Bocanegra, A.D. Ballarini, O.A. Scelza, S.R. de Miguel, The influence of the synthesis routes of MgAl2O4 on its properties and behaviour as support of dehydrogenation catalysts, Mater. Chem. Phys. 111 (2008) 534–541.
20. J. Bai, J. Liu, C. Li, G. Li, Q. Du, Mixture of fuels approach for solution combustion synthesis of nanoscale MgAl2O4 powders, Advanced Powder Technology 22 (2011) 72-76.
21. M. Kobayashi, Y. Usuki, M. Ishii, N. Senguttuvan, K. Tanji, M. Chiba, A. Hark, H. Takano, M. Nikl, P. Bohacek, A. Cecilia, M. Diemoz, A. Vedda, M. Martini, Scintillation characteristics of PbWO4 single crystals doped with Th, Zr, Ce, Sb and Mn ions, Nucl. Instrum. Methods Phys. Res. A 465 (2001) 428-439.
22. V.S. Vinila, R. Jacob, A. Mony, H.G. Nair, S. Issac, S. Rajan, A.S. Nair, J. Isac, XRD Studies on Nano Crystalline Ceramic Superconductor PbSrCaCuO at Different Treating Temperatures, Crystal Structure Theory and Applications 3 (2014) 1-19.
23. A.K.M. Akther Hossain, S.T. Mahmud, M. Seki, T. Kawai, H. Tabata, Structural, electrical transport, and magnetic properties of Ni1–xZnxFe2O4, J. Magn. Magn. Mater. 312 (2007) 210-219.
24. G. Li, L. Li, J. Boerio-Goates, B.F. Woodfield, High Purity Anatase TiO2 Nanocrystals: Near Room-Temperature Synthesis, Grain Growth Kinetics, and Surface Hydration Chemistry, J. Am. Chem. Soc. 127 (2005) 8659-8666.
25. D. Simeone, C. Dodane-Thiriet, D. Gosset, P. Daniel, M. Beauvy, Order–disorder phase transition induced by swift ions in MgAl2O4 and ZnAl2O4 spinels, J. Nucl. Mater. 300 (2002) 151-160.
26. K.E. Sickafus, Comment on 'Order-disorder phase transition induced by swift ions in MgAl2O4 and ZnAl2O4 spinels' by D. Simeone et al., J. Nucl. Mater. 300 (2002) 151-160, J. Nucl. Mater. 312 (2003) 111-123.
27. A.I. Gusev, A.A. Rempel, Nanocrystalline Materials. Cambridge International Science Publication Cambridge, 2004.
28. A.K. Adak, S.K. Saha, P. Pramanik, Synthesis and characterization of MgAl2O4 spinel by PVA evaporation technique, J. Mater. Sci. Lett. 16 (1997) 234-235.
29. H. Toroya, M. Yoshimura, Somiy, Calibration Curve for Quantitative Analysis of the Monoclinic-Tetragonal ZrO2 System by X-Ray Diffraction, J. Am. Ceram. Soc. 67 (1984) C119–C121.
30. P. Barpanda, S.K. Behera, P.K. Gupta, S.K. Pratihar, S. Bhattacharya, Chemically induced order disorder transition in magnesium aluminium spinel, J. Eur. Ceram. Soc. 26 (2006) 2603–2609.

31. C. Suryanarayana, C.C. Koch, Nanocrystalline materials–Current research and future directions, Hyperfine Interaction 130 (2000) 5-44.
32. K. Vivekanandan, S. Selvasekarapandian, P. Kolandaivel, Raman and FT-IR studies of Pb4(NO3)2(PO4)2·2H2O crystal, Mater. Chem. Phys. 39 (1995) 284-289.
33. M.A. Ulibarri, C. Barriga, J. Cornejo, Kinetics of the thermal dehydration of some layered hydroxycarbonates, Thermochim. Acta 135 (1988) 231–236.
34. P. Aghamkar, S. Duhan, M. Singh, N. Kishore, P.K. Sen, Effect of thermal annealing on Nd2O3-doped silica powder prepared by the solgel process, J. Sol-Gel Sci. Technol. 46 (2008)17–22.
35. R.V. Prikhod'ko, M.V. Sychev, I.M. Astrelin, K. Erdmann, A. Mangel, R.A. Van Santen, Synthesis and Structural Transformations of Hydrotalcite-like Materials Mg3Al and Zn3Al, Russ. J. Appl. Chem. 74 (2001) 1621-1626.
36. F. Meyer, R. Hempelmann, S. Mathur, M. Veith, Microemlusion mediated sol-gel synthesis of nano scaled MAl2O4 (M= Co, Ni, Cu) spinels from single-Source Heterobimetallic Alkoxide precursor, J. Mater. Chem. 9 (1999) 1755-1763.
37. Fa-tang Li, Ye Zhaoa, Ying Liua, Ying-juan Haoa, Rui-hong Liua, Di-shun Zhaob, Solution combustion synthesis and visible light-induced photocatalytic activity of mixed amorphous and crystalline MgAl2O4 nanopowders, Chem. Eng. J. 173 (2011) 750–759.
38. Jr E.H. Walker, J.W. Owens, M. Etienne, D. Walker, The novel low temperature synthesis of nanocrystalline MgAl2O4 spinel using "gel" precursors, Mater. Res. Bull. 37 (2002) 1041-1050.

**Cite this Article**

Dr. Shyam Sunder, Dr. Wazir Singh, "Thermal Evolution of Magnesium Aluminate Spinel Nanoparticles Prepared By Coprecipitation Technique", International Journal of Scientific Research in Science, Engineering and Technology (IJSRSET), Online ISSN : 2394-4099, Print ISSN : 2395-1990, Volume 4 Issue 6, pp. 294-305, January-February 2018.

Journal URL : http://ijsrset.com/IJSRSET184480